

Diffusion-weighted imaging in the assessment of tumour grade in endometrial cancer

¹N BHARWANI, MRCP, FRCR, ²M E MIQUEL, PhD, ¹A SAHDEV, MRCP, FRCR, ¹P NARAYANAN, MRCP, FRCR, ¹G MALIETZIS, MBBS, MScS, ¹R H REZNEK, FRCP, FRCR and ¹A G ROCKALL, MRCP, FRCR

¹Department of Imaging and ²Department of Clinical Physics, Barts and The London NHS Trust, London, UK

Objective: Endometrial cancer is the most common gynaecological malignancy in developed countries. Histological grade and subtype are important prognostic factors obtained by pipelle biopsy. However, pipelle biopsy “samples” tissue and a high-grade component that requires more aggressive treatment may be missed. The purpose of the study was to assess the use of diffusion-weighted MRI (DW-MRI) in the assessment of tumour grade in endometrial lesions.

Method: 42 endometrial lesions including 23 endometrial cancers and 19 benign lesions were evaluated with DW-MRI (1.5T with multiple *b*-values between 0 and 750 s mm⁻²). Visual evaluation and the calculation of mean and minimum apparent diffusion coefficient (ADC) value were performed and correlated with histology.

Results: The mean and minimum ADC values for each histological grade were 1.02 ± 0.29 × 10⁻³ mm² s⁻¹ and 0.74 ± 0.24 × 10⁻³ mm² s⁻¹ (grade 1), 0.88 ± 0.39 × 10⁻³ mm² s⁻¹ and 0.64 ± 0.36 × 10⁻³ mm² s⁻¹ (grade 2), and 0.94 ± 0.32 × 10⁻³ mm² s⁻¹ and 0.72 ± 0.36 × 10⁻³ mm² s⁻¹ (grade 3), respectively. There was no statistically significant difference between tumour grades. However, the mean ADC value for endometrial carcinoma was 0.97 ± 0.31, which was significantly lower (*p* < 0.0001) than that of benign endometrial pathology (1.50 ± 0.14). Applying a cut-off mean ADC value of less than 1.28 × 10⁻³ mm² s⁻¹ we obtained a sensitivity, specificity, positive predictive value and negative predictive value for malignancy of 87%, 100%, 100% and 85.7%, respectively.

Conclusion: Tumour mean and minimum ADC values are not useful in differentiating histological tumour grade in endometrial carcinoma. However, mean ADC measurement can provide useful information in differentiating benign from malignant endometrial lesions. This information could be clinically relevant in those patients where pre-operative endometrial sampling is not possible.

Received 17 October 2010

Revised 2 January 2011

Accepted 18 January 2011

DOI: 10.1259/bjr/14980811

© 2011 The British Institute of Radiology

Endometrial carcinoma is the commonest gynaecological malignancy in developed countries [1, 2]. The majority of patients present with intermenstrual or post-menopausal bleeding, with approximately 70–80% having early (Stage I) disease at presentation [1, 3]. Despite the relatively high incidence, endometrial cancer is not a common cause of cancer death with a 5 year survival of approximately 80% when all stages are considered together [4].

The most important prognostic indicators in endometrial cancer are FIGO (International Federation of Gynecology and Obstetrics) stage, lymphovascular invasion, histological subtype and grade, and the presence of lymph node metastases [4–8]. FIGO staging of endometrial cancer is a surgico-pathological staging system that includes total hysterectomy, bilateral salpingo-oophorectomy and peritoneal washings with full pelvic lymphadenectomy [9]. The overall rate of lymph node involvement in endometrial cancer is low (5–8%) and lymphadenectomy carries a reported complication risk

of up to 17–19% [10, 11], which is particularly marked in patients who are at high surgical risk, such as those who are obese, diabetic or suffer from ischaemic heart disease [12]. As a result, only around 30% of endometrial cancer patients undergo lymphadenectomy in the USA as a whole, increasing to 48.3% in specialised cancer centres [13]. The role of lymphadenectomy in the management of endometrial cancer is currently an area of controversy in gynaecological oncology with no clear evidence regarding the survival benefits associated with the procedure [14–17]. However, in patients who are at high risk of nodal metastases most centres continue to perform lymphadenectomy.

Accurate pre-operative identification of patients at high risk of nodal metastases would allow the selection of patients for lymphadenectomy, while those at low risk could be treated with simple hysterectomy. Histological tumour grade is a strong predictor of nodal invasion and thereby prognosis in endometrial cancer [18, 19]. In patients with FIGO Stage 1 disease, grade 1 or grade 2 histology carries a less than 10% risk of nodal metastases. However, grade 3 histology carries an overall risk of 18% in Stage 1 disease, which increases to 34% when considering patients with deep myometrial invasion [18, 19]. Pre-operative cytology from pipelle or curettage

Address correspondence to: Dr Nishat Bharwani, Imaging Department (Room 3), King George V Wing (Ground Floor), St Bartholomew's Hospital, West Smithfield, London EC1A 7BE, UK. E-mail: nishat.bharwani@nhs.net

specimens only samples the endometrial tissue and therefore does not always provide accurate assessment [20, 21]. In a study of patients with grade 1 histology pre-operatively 19% were upgraded following surgical resection [22].

Diffusion-weighted MRI (DW-MRI) is a functional imaging technique that looks at the Brownian motion of water in tissues. In biological tissues this is restricted by interactions with cell membranes and macromolecules on a microscopic level. Increased tissue cellularity, as seen in tumours, restricts Brownian motion, which can be quantified by calculation of the apparent diffusion coefficient (ADC) [23].

Previous publications have demonstrated that endometrial carcinoma may be distinguished from normal endometrium on DW-MRI [24–30]. It has also been suggested that DW-MRI may be useful in the pre-operative assessment of tumour grade [26, 31]. The purpose of this study is to determine if there is a correlation between histological tumour grade and ADC value in endometrial cancer.

Methods and materials

The study protocol was approved by the local institutional review board. All patients gave permission for the use of their anonymised data for research purposes at the time of their scan.

Study population

This retrospective study was performed between April 2007 and June 2009. The study group consisted of 23 female patients (mean age: 62.4 years; age range: 44–92 years) with histologically proven endometrial cancer who underwent pelvic MRI with diffusion-weighted sequences at our institution. MRI was performed to assess the extent of tumour invasion and local staging following histological confirmation of endometrial cancer at curettage or pipelle biopsy.

For comparison, analysis was performed on 19 female patients (mean age: 46 years; age range: 19–89 years) undergoing pelvic MRI for other indications. Two

patients underwent MRI following complete hysteroscopic removal of a malignant endometrial polyp where subsequent hysterectomy showed no residual tumour (therefore MRI performed after hysteroscopy imaged benign endometrium only). The indications for MRI in the remaining 17 patients were menstrual abnormality/post-menopausal bleeding ($n = 4$), follow-up for previous borderline ovarian tumour ($n = 3$), adnexal mass characterisation ($n = 5$), cervical cancer with no evidence of endometrial involvement ($n = 4$) and screening for familial paraganglioma syndrome ($n = 1$).

MR scanning protocol

All participants were imaged using a 1.5 Tesla Philips Achieva MRI scanner (Philips Medical Systems, Best, the Netherlands) in conjunction with a 4-element torso phased array coil.

For all sequences, the field of view (FOV) and number of slices were optimised for each individual patient to cover the anatomy of interest. All participants underwent axial T_1 weighted, axial T_2 weighted and sagittal T_2 weighted turbo spin-echo (TSE) sequences and diffusion-weighted scans. In addition, further axial oblique T_2 weighted TSE sequences (obtained in a plane perpendicular to the long axis of the uterine body) and contrast medium enhanced imaging were performed in those patients with endometrial cancer. The contrast enhanced sequences comprised axial oblique pre- and post-gadolinium (10 ml Dotarem (279.32 mg ml⁻¹), Guebert, Paris, France) T_1 weighted fat saturated sequences, including a dynamic perfusion run in the sagittal plane with five dynamic acquisitions. Details of sequence parameters are given in Table 1.

DW-MRI images were obtained using a multislice single-shot spin-echo type echo planar sequence under free breathing. Diffusion images were synthesised isotropic with the mean of three orthogonal directions being taken. The following parameters were used: repetition time (TR) 5300–5800 ms, time to echo (TE) 62 ms, echo planar imaging (EPI) factor 60, number of acquisitions (NSA) 3, FOV 400–450 mm, rectangular FOV (RFOV) 75%, matrix 112 × 256, 32 slices, slice thickness 6 mm, slice gap 1 mm, 2 to 6 b -values between 0 and 1000 s mm⁻². In

Table 1. MRI scan parameters

	T_2 weighted axial TSE	T_2 weighted sagittal TSE	T_2 weighted oblique TSE	T_1 weighted axial TSE	T_1 weighted fat saturated	Dynamic scan
TE (ms)	100	100	100	18	18	1.8
TR (ms)	>3300	>3300	5362	500–600	621	3.7
FOV	375–450	240–300	240	375–450	240–320	280–320
RFOV (%)	70–75	100	91	70	100	100
Slice thickness (mm)	6	4	3	6	5	8
Slice gap (mm)	0.6–1	0.4–1	0.3	0.6–1	0.5	–4
Number of slices	32	25–30	24–30	32	20	40
NSA	6	6	6	3	3	6
Matrix	294 × 512	256–282 × 512	205 × 256	320 × 512	205 × 512	166 × 256
Turbo factor	15	14–15	16	3–4	3	60
Flip angle (degrees)	90	90	90	90	90	10
Fat saturation	None	None	None	None	SPIR	SPIR
Number of dynamics	1	1	1	1	1	5

TSE, turbo spin-echo; TE, echo time; TR, repetition time; FOV, field of view; RFOV, rectangular field of view; NSA, number of acquisitions; SPIR, spectral pre-saturation inversion recovery.

6 patients the b -values used were 0, 225, 451, 676, 901 s mm^{-2} ; in 1 patient only 2 b -values were obtained ($b = 0$ and $b = 1000$) and in the remaining 35 patients the b -values used were 0, 50, 100, 250, 500, 750 s mm^{-2} . The b -values used during the study changed owing to optimisation of the DW-MRI protocols applied at our institution over the period. ADC maps were generated using the software on the Philips Achieva MRI scanner (software package 1.5.4.3) using all available b -values.

Image analysis

Images were retrospectively reviewed by two radiologists, independently. Both readers were experienced in reporting gynaecological oncology MRI (Reader 1 had 10 years experience; Reader 2 had 1.5 years experience). It was not possible to fully blind the readers as many patients with endometrial carcinoma had an obvious endometrial mass. Readers were blinded to the grade and histological subtype of the endometrial cancer but knew the age and menopausal status. In patients with benign endometrial pathology the readers were blinded to the endometrial histology when available.

All sequences performed were available to the readers at the time of image analysis. Each reader localised the endometrial tumour using T_2 weighted and dynamic gadolinium images. These appearances were then correlated with the DW-MRI sequences using the available b -values and the corresponding ADC map. The software used for analysis did not have the capability for volumetric analysis. Once the tumour was localised, the largest possible region of interest (ROI) was drawn within the tumour on a single image slice. Care was taken to avoid contamination of this ROI by adjacent normal endometrium or myometrium or by areas of fluid/necrosis within the endometrial cavity (Figure 1). In smaller lesions this was sometimes difficult; however, in our cohort we did not need to exclude any patients because of small ROI size. In patients with no visible endometrial mass, the ROI was positioned over the largest possible area of endometrium

on a single slice. The mean and minimum ADC values (in millimetres squared per second) were calculated by the software on the Philips workstation using the following formula:

$$\text{ADC} = (1/(b_x - b_0)) \ln(S_0/S_x)$$

where S_x and S_0 represent the signal intensity of the images acquired at b_x and b_0 .

Statistical analysis

Mean and minimum ADC values between tumour grades and between benign and malignant tissue were compared using a one-way ANOVA (analysis of variance) with $p < 0.05$ considered significant using the Statistical Package for Social Sciences statistical package version 18 (SPSS Inc, Chicago, IL). Interobserver variability was evaluated using the Analyse-it statistical package (Analyse-it Software Ltd, Leeds, UK) in conjunction with Microsoft Excel (Microsoft Corporation, Redmond, WA) to generate a Bland-Altman plot.

Histological validation

In patients with endometrial carcinoma, the histological subtype and grade was confirmed following hysterectomy in 20 cases. In the remaining three patients, only pipelle or curettage samples were available as the patients were unfit for surgery.

In patients without endometrial cancer, histological validation of endometrial tissue was available in 12 patients (7 from pipelle or curettage samples and 5 from hysterectomy specimens). In the remaining 7 patients it was presumed that no endometrial abnormality was present as the patients were asymptomatic and were having MRI scans for unrelated clinical indications. In these patients the MRI scans were reviewed prior to inclusion to ensure that there were no imaging features to suggest endometrial pathology.

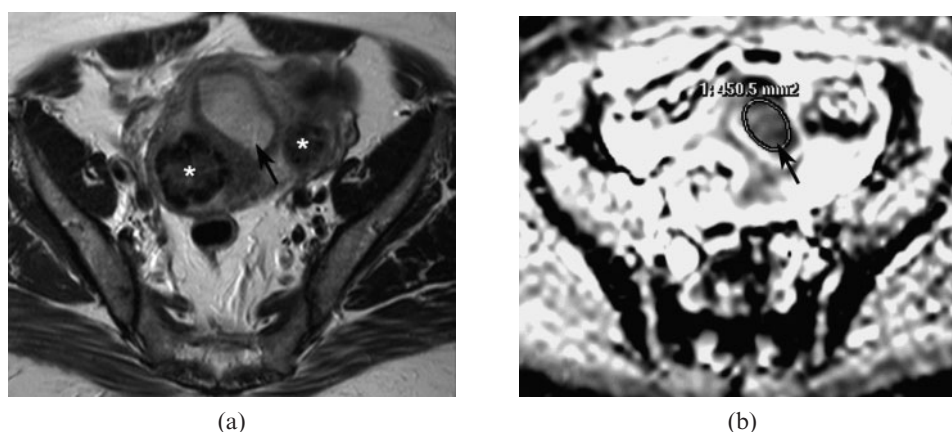


Figure 1. (a) Axial T_2 weighted image showing an intermediate signal intensity endometrial carcinoma expanding the endometrial cavity (arrow). (b) Apparent diffusion coefficient (ADC) map at a corresponding level showing the low signal intensity tumour (arrow). The largest possible region of interest (ROI) is drawn around the tumour on the ADC map without contamination from adjacent normal endometrium or myometrium. *Fibroid.

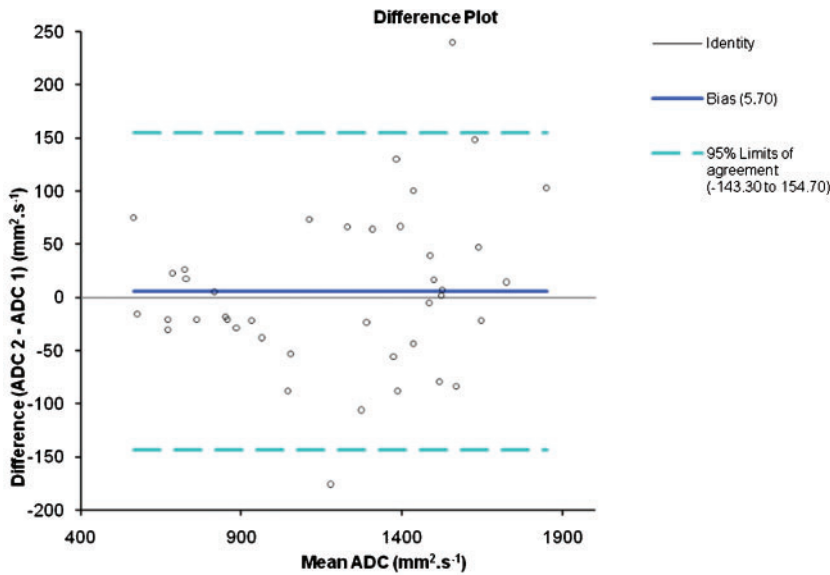


Figure 2. Bland–Altman plot illustrating the interobserver variability between Reader 1 and Reader 2. The 95% confidence interval for the data is -143.3 to $+154.7$ $\text{mm}^2 \text{ s}^{-1}$.

Results

Histopathology

Of the 23 patients with endometrial carcinoma, 18 had endometrioid adenocarcinoma (12 grade 1; 4 grade 2; 2 grade 3); 2 had mixed endometrioid adenocarcinoma and serous papillary carcinoma; 2 had serous papillary carcinomas and 1 had clear cell carcinoma on histology. Clear cell and serous papillary carcinomas are considered to be aggressive histological subtypes and are associated with a worse prognosis than endometrioid adenocarcinoma [32–34]. Therefore in surgical planning, and for the purpose of this study, they are taken to represent the equivalent of grade 3 endometrioid adenocarcinomas, giving a total of 7 patients with grade 3 histopathology.

Of the 19 patients with non-malignant endometrial tissue, 2 had endometrial hyperplasia, 2 were in the proliferative phase, 2 were benign polyps and 2 were reported as benign endometrial tissue. No definitive endometrial histology was available in 7 presumed benign cases.

Interobserver variability

Interobserver variability in mean ADC value measurement was assessed by generating a Bland–Altman plot (Figure 2). This plot showed good agreement with the mean difference in values between the 2 readers ranging from -0.14 to $+0.15 \times 10^{-3} \text{ mm}^2 \text{ s}^{-1}$.

Diffusion-weighted MRI analysis

DW-MR images were viewed in conjunction with conventional MRI for anatomical correlation of the endometrium. On DW-MRI, the signal intensity of the endometrial tumour increased with increasing *b*-value and the tumours were bright in contrast to the dark background on the *b* = 750 images with corresponding low signal intensity (restricted diffusion) on the ADC map (Figure 3). In some cases, heterogeneity of signal intensity was seen.

ADC analysis

One patient in the non-malignant group was excluded from the ADC analysis as there was significant patient

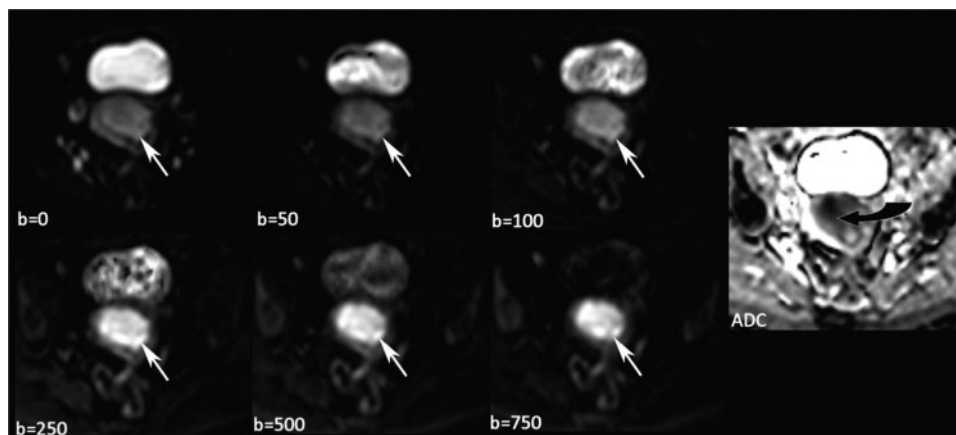


Figure 3. Sequential *b*-values showing an endometrial carcinoma becoming brighter with increasing *b*-value (white arrows). The apparent diffusion coefficient (ADC) map generated using all six *b*-values shows the tumour returning low signal intensity (curved black arrow) in keeping with restricted diffusion.

Table 2. Mean apparent diffusion coefficient (ADC) value and standard deviation for endometrial cancer and normal endometrium for Reader 1 and Reader 2

		Mean ADC ($\times 10^{-3} \text{ mm}^2 \text{ s}^{-1}$)	Standard deviation	Minimum value ($\times 10^{-3} \text{ mm}^2 \text{ s}^{-1}$)	Maximum value ($\times 10^{-3} \text{ mm}^2 \text{ s}^{-1}$)
Endometrial cancer ($n=23$)	Reader 1	0.97	0.31	0.53	1.66
	Reader 2	0.96	0.30	0.57	1.64
Normal endometrium ($n=18$)	Reader 1	1.49	0.14	1.30	1.80
	Reader 2	1.52	0.17	1.22	1.90

movement between acquisition of diffusion data at the six b -values and the ADC map was, therefore, difficult to interpret and the appropriate placement of a ROI was impossible.

The mean ADC value and standard deviation in cases of endometrial cancer ($n=23$) and normal endometrium ($n=18$) for both readers are given in Table 2. There was minimal variability between the observers so the values obtained by Reader 1 were used for subsequent analysis. ROI size ranged from 53.6 mm^2 to 2718.2 mm^2 with a mean of $213.6 \pm 499.37 \text{ mm}^2$.

The mean and minimum ADC value for each histological grade was $1.02 \pm 0.29 \times 10^{-3} \text{ mm}^2 \text{ s}^{-1}$ and $0.74 \pm 0.24 \times 10^{-3} \text{ mm}^2 \text{ s}^{-1}$ (grade 1), $0.88 \pm 0.39 \times 10^{-3} \text{ mm}^2 \text{ s}^{-1}$ and $0.64 \pm 0.36 \times 10^{-3} \text{ mm}^2 \text{ s}^{-1}$ (grade 2), and $0.94 \pm 0.32 \times 10^{-3} \text{ mm}^2 \text{ s}^{-1}$ and $0.72 \pm 0.36 \times 10^{-3} \text{ mm}^2 \text{ s}^{-1}$ (grade 3), respectively. These ADC values show a trend toward lower values with increasing tumour grade; however, there was considerable overlap and no statistically significant difference was demonstrated between tumour grades for mean ADC value or for minimum ADC value (Figure 4 and 5). Further sub-group analysis of the 35 patients imaged using the same b -values did not demonstrate any significant difference between tumour grades.

There was a statistically significant difference between the mean and minimum ADC values of benign ($1.49 \pm 0.14 \times 10^{-3} \text{ mm}^2 \text{ s}^{-1}$ and $1.16 \pm 0.20 \times 10^{-3} \text{ mm}^2 \text{ s}^{-1}$, respectively) and malignant ($0.97 \pm 0.31 \times 10^{-3} \text{ mm}^2 \text{ s}^{-1}$

and $0.72 \pm 0.30 \times 10^{-3} \text{ mm}^2 \text{ s}^{-1}$, respectively) endometrial pathology ($p < 0.0001$). When a cut-off mean ADC value of $1.28 \times 10^{-3} \text{ mm}^2 \text{ s}^{-1}$ is applied to our data a sensitivity of 86.96% (20/23), specificity of 100% (18/18), positive predictive value (PPV) of 100% (20/20), negative predictive value (NPV) of 85.71% (18/23), and an accuracy of 92.68% (38/41) for malignancy is obtained (Figure 6).

Discussion

MRI is a well-established imaging technique for the pre-operative evaluation of endometrial carcinoma [35, 36]. However, conventional MRI sequences cannot differentiate between carcinoma, endometrial hyperplasia or benign polyps and histological confirmation is required [35].

In this study, functional imaging with DW-MRI shows restriction of movement of water molecules in endometrial cancer with increased signal intensity particularly at high b -values ($b > 500 \text{ s mm}^{-2}$) and corresponding low signal intensity on ADC maps. This is in agreement with published reports of decreased ADC values in endometrial cancer [24–30]. It must be stressed that the DW-MRI and ADC appearances need to be correlated with conventional T_1 and T_2 weighted imaging owing to the relatively poor resolution of DW-MRI for accurate anatomical correlation.

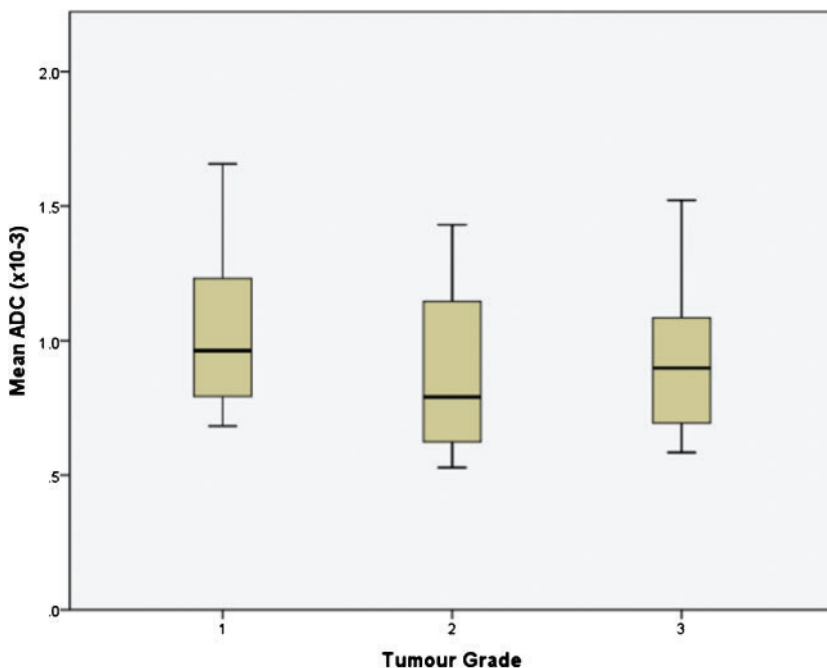


Figure 4. Box-and-whisker plot showing the mean ADC values ($\times 10^{-3} \text{ mm}^2 \text{ s}^{-1}$) of endometrial cancers in each histological grade. The central horizontal line within the box represents the mean value; the bottom and top edges of the box indicate the 25th and 75th percentiles and the vertical line indicates the range of the data. The mean ADC value for endometrial cancer showed a trend for being lower in grade 3 tumours than grade 1; however, this did not reach statistical significance.

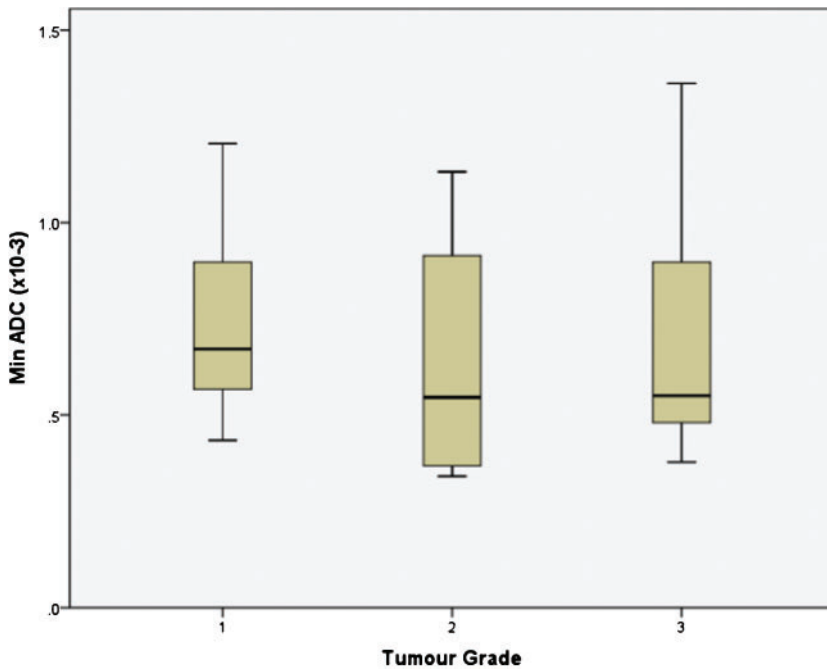


Figure 5. Box-and-whisker plot showing the minimum apparent diffusion coefficient (ADC) values ($\times 10^{-3} \text{ mm}^2 \text{ s}^{-1}$) for different grades of endometrial carcinoma. The central horizontal line within the box represents the mean value; the bottom and top edges of the box indicate the 25th and 75th percentiles and the vertical line indicates the range of the data. The minimum ADC value for endometrial cancer showed a trend for being lower in grade 3 tumours than grade 1; however, this did not reach statistical significance.

Calculation of ADC maps from the source diffusion images allows quantitative analysis of water diffusivity on a microscopic level within tissues. Restriction of diffusion is thought to be due to dense cellularity and larger cell diameter [23]; with increasing tumour cellularity and architectural distortion there is a reduction in the extracellular space, which also becomes increasingly tortuous. High-grade endometrial adenocarcinomas typically have a higher cellular density and would therefore be expected to have lower ADC values than low-grade tumours. However, in our cohort we found considerable overlap in mean ADC values between the different tumour grades making estimation of histological grade impossible. We postulated that tumour heterogeneity may account for this overlap and went on to assess the

minimum ADC value obtained from the tumour ROI to quantify the most restricted part of the ROI. The rationale for measuring minimum ADC was extrapolated from the use of maximum standardised uptake value (SUV_{max}) in assessment of tumour grade in endometrial cancer on PET-CT [37]. Once again there was no statistically significant difference between tumour grades. The use of minimum ADC values in body DW-MRI can be subject to contamination by noise, which is likely to explain this result. Histogram analysis looking at the spread of ADC values within the selected ROI may overcome this problem. The lack of correlation between ADC value (minimum or mean) and tumour grade may be a reflection of the fact that cellularity is only one of the factors used to determine tumour grade at histological

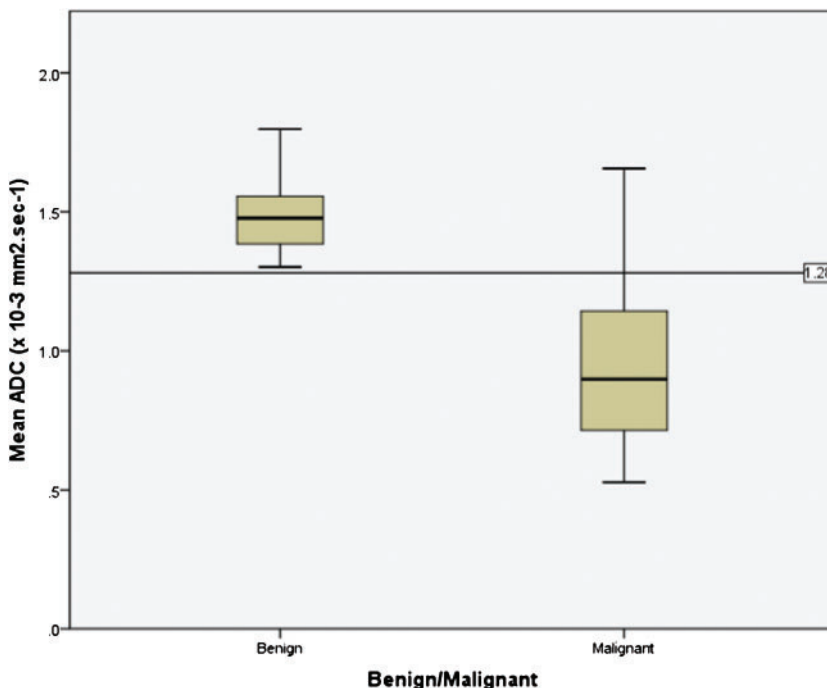


Figure 6. Box-and-whisker plot showing the mean ADC values ($\times 10^{-3} \text{ mm}^2 \text{ s}^{-1}$) for endometrial cancer (malignant) and benign endometrial pathology. The central horizontal line within the box represents the mean value; the bottom and top edges of the box indicate the 25th and 75th percentiles and the vertical line indicates the range of the data. The ADC values for endometrial cancer were significantly lower than those of benign endometrium ($p < 0.0001$). The cut-off line drawn at an ADC value of $1.28 \times 10^{-3} \text{ mm}^2 \text{ s}^{-1}$ divides the benign and malignant endometrial tissue yielding a sensitivity, specificity and accuracy of 87%, 100% and 93% for malignant tissue respectively. Using this cut-off value, three patients with malignant histology lie above the line.

Table 3. Statistical analysis of our data using suggested mean apparent diffusion coefficient (ADC) cut-off values from the literature

Authors	<i>b</i> -values (s mm ²) applied in study	Suggested cut-off mean ADC value ($\times 10^{-3}$ mm ² s ⁻¹)	Sensitivity (%)	Specificity (%)	PPV (%)	NPV (%)	Accuracy (%)
Kilickesmez et al [28]	0, 500, 1000	1.05	60.1	100	100	66.7	78
Fujii et al [24]	0, 1000	1.15	73.9	100	100	75	85.4
Takeuchi et al [30]	0, 800	1.2	78.3	100	100	78.3	87.8
This study	0, 50, 100, 250, 500, 750 (<i>n</i> = 35)*	1.28	87	100	100	85.7	92.7

PPV, positive predictive value; NPV, negative predictive value. **b*-values of 0, 225, 451, 676, 901 s mm² in *n* = 6 patients and *b*-values of 0, 1000 s mm² in *n* = 2 patients.

analysis. Other factors important in grading, such as nuclear atypia, are not assessed on DW-MRI.

Our results show that both the mean and minimum ADC values of endometrial carcinoma are significantly lower than those of benign endometrial histology. This finding is in agreement with other published reports; in one study there was no overlap in mean ADC value between the two groups [26] and in other studies only a small degree of overlap in values with the difference remaining statistically significant [24, 28–30]. Previous studies have suggested mean ADC cut-off values that can be used to predict malignancy in endometrial lesions [24, 28, 30]. These mean ADC cut-off values range from 1.05×10^{-3} to 1.2×10^{-3} mm² s⁻¹. When applied to the data from our cohort of patients we achieved an accuracy of 78–87.8% (Table 3). However, applying our own cut-off ADC value of 1.28×10^{-3} mm² s⁻¹ we achieved sensitivity, specificity, PPV, NPV and accuracy rates of 87%, 100%, 100%, 85.7% and 92.7%, respectively. It is difficult to establish a universal threshold ADC value above which malignancy should be suggested owing to variations in the MRI system used and the number of *b*-values used to generate the ADC map. The previously published cut-off values were obtained using 1.5T Siemens (Siemens AG, Erlangen, Germany) systems in two studies [24, 28], while the third study used both 1.5T and 3T GE (GE Healthcare, Milwaukee, WI) systems [30] and used 2 or 3 *b*-values between 0 and 1000 s mm⁻². The threshold value with the greatest accuracy for our 1.5T Philips system (1.28×10^{-3} mm² s⁻¹) is of the same order of magnitude as the prior values and the variation between values is up to 0.23×10^{-3} mm² s⁻¹.

In our study two patients had MRI performed following hysteroscopic removal of a malignant endometrial polyp (grade 1 endometrial adenocarcinoma in both cases). In these patients the mean ADC values measured for endometrial tissue post-polypectomy were 1.4×10^{-3} mm² s⁻¹ and 1.6×10^{-3} mm² s⁻¹. By applying our proposed cut-off value we would have been able to predict that neither of these patients had residual tumour present as both values lie in the benign range. The ability to make this prediction would probably not prevent surgery in patients with positive pre-operative histology but could allow triage of the patient to a less radical surgical approach. Further clinical application of a benign/malignant threshold would be for patients for whom it is difficult to obtain pre-operative histology (e.g. cervical stenosis) where an ADC value suggesting malignancy could prevent repeated attempts at sampling

and allow earlier management planning in these difficult cases.

There are some limitations to our study. Firstly, this preliminary cohort of patients is relatively small. Secondly, in some of our benign group we presumed that there was no endometrial pathology present as patients were asymptomatic and were being imaged for unrelated reasons. Ideally, histological confirmation should be available for all patients. Some of the tumours we analysed were small and only present on two contiguous slices. In these cases the ROI was placed on the slice with the largest area of visible tumour; however, as tumour was not present on the section above and below, it is possible that the data are subject to some partial volume effect. Further evaluation of these patients did not show them to be outliers in our data and therefore this is not felt to have been a significant problem in our cohort. Finally, a small number of patients (7 of 42) were imaged with different *b*-values owing to the retrospective nature of our study. Comparison with other studies is also difficult as centres use different *b*-values in their DW-MRI protocols and this requires collaboration and universal recommendations.

To validate our suggested threshold value, further prospective studies with a larger cohort of patients should be undertaken. Assessment on different MR systems, both at 1.5 and 3T, is also required to test reproducibility.

Conclusion

DWI with the measurement of mean ADC value is useful in demonstrating the presence of endometrial cancer. However, histological tumour grades 1 to 3 could not be distinguished based on the mean or minimum ADC value of the tumour. The application of a mean ADC threshold less than 1.28×10^{-3} mm² s⁻¹ gives 92.7% accuracy in predicting the presence of endometrial cancer rather than benign endometrial pathology, which is particularly relevant in those patients for whom it is difficult to obtain pre-operative histology.

References

1. Cancer UK Database. 2010 July. Available from: <http://info.cancerresearchuk.org/cancerstats/types/uterus/>.
2. Jemal A, Siegel R, Ward E, Hao Y, Xu J, Thun MJ. Cancer Statistics, 2009. *CA Cancer J Clin* 2009.
3. SEER Cancer Database. 2010 July. Available from: <http://seer.cancer.gov/statfacts/html/corp.html>.

4. Amant F, Moerman P, Neven P, Timmerman D, Van Limbergen E, Vergote I. Endometrial cancer. *Lancet* 2005; 366:491–505.
5. Kinkel K, Kaji Y, Yu KK, Segal MR, Lu Y, Powell CB et al. Radiologic staging in patients with endometrial cancer: a meta-analysis. *Radiology* 1999;212:711–18.
6. Koyama T, Tamai K, Togashi K. Staging of carcinoma of the uterine cervix and endometrium. *Eur Radiol* 2007;17: 2009–19.
7. Larson DM, Connor GP, Broste SK, Krawisz BR, Johnson KK. Prognostic significance of gross myometrial invasion with endometrial cancer. *Obstet Gynecol* 1996;88:394–8.
8. Orezza JP, Sioletic S, Olawaiye A, Oliva E, del Carmen MG. Stage II endometrioid adenocarcinoma of the endometrium: clinical implications of cervical stromal invasion. *Gynecol Oncol* 2009;113:316–23.
9. Pecorelli S. Revised FIGO staging for carcinoma of the vulva, cervix, and endometrium. *Int J Gynaecol Obstet* 2009;105:103–4.
10. McMeekin DS, Lashbrook D, Gold M, Scribner DR, Kamelle S, Tillmanns TD et al. Nodal distribution and its significance in FIGO stage IIIc endometrial cancer. *Gynecol Oncol* 2001;82:375–9.
11. Morrow CP, Bundy BN, Kurman RJ, Creasman WT, Heller P, Homesley HD et al. Relationship between surgical-pathological risk factors and outcome in clinical stage I and II carcinoma of the endometrium: a Gynecologic Oncology Group study. *Gynecol Oncol* 1991;40:55–65.
12. Tozzi R, Malur S, Koehler C, Schneider A. Analysis of morbidity in patients with endometrial cancer: is there a commitment to offer laparoscopy? *Gynecol Oncol* 2005;97: 4–9.
13. Partridge EE, Shingleton HM, Menck HR. The National Cancer Data Base report on endometrial cancer. *J Surg Oncol* 1996;61:111–23.
14. Dowdy SC, Mariani A. Lymphadenectomy in endometrial cancer: when, not if. *Lancet* 2010;375:1138–40.
15. Benedetti PP, Basile S, Maneschi F, Alberto LA, Signorelli M, Scambia G et al. Systematic pelvic lymphadenectomy vs. no lymphadenectomy in early-stage endometrial carcinoma: randomized clinical trial. *J Natl Cancer Inst* 2008; 100:1707–16.
16. Kitchener H, Swart AM, Qian Q, Amos C, Parmar MK. Efficacy of systematic pelvic lymphadenectomy in endometrial cancer (MRC ASTEC trial): a randomised study. *Lancet* 2009;373:125–36.
17. Todo Y, Kato H, Kaneuchi M, Watari H, Takeda M, Sakuragi N. Survival effect of para-aortic lymphadenectomy in endometrial cancer (SEPAL study): a retrospective cohort analysis. *Lancet* 2010;375:1165–72.
18. Boronow RC, Morrow CP, Creasman WT, Disaia PJ, Silverberg SG, Miller A et al. Surgical staging in endometrial cancer: clinical-pathologic findings of a prospective study. *Obstet Gynecol* 1984;63:825–32.
19. Creasman WT, Morrow CP, Bundy BN, Homesley HD, Graham JE, Heller PB. Surgical pathologic spread patterns of endometrial cancer. A Gynecologic Oncology Group Study. *Cancer* 1987;60:2035–41.
20. Dubinsky TJ, Parvey HR, Maklad N. The role of transvaginal sonography and endometrial biopsy in the evaluation of peri- and postmenopausal bleeding. *AJR Am J Roentgenol* 1997;169:145–9.
21. Park BK, Kim B, Park JM, Ryu JA, Kim MS, Bae DS et al. Differentiation of the various lesions causing an abnormality of the endometrial cavity using MR imaging: emphasis on enhancement patterns on dynamic studies and late contrast-enhanced T_1 -weighted images. *Eur Radiol* 2006;16:1591–8.
22. Ben Shachar I, Pavelka J, Cohn DE, Copeland LJ, Ramirez N, Manolitsas T et al. Surgical staging for patients presenting with grade 1 endometrial carcinoma. *Obstet Gynecol* 2005;105:487–93.
23. Koh DM, Collins DJ. Diffusion-weighted MRI in the body: applications and challenges in oncology. *AJR Am J Roentgenol* 2007;188:1622–35.
24. Fujii S, Matsusue E, Kigawa J, Sato S, Kanasaki Y, Nakanishi J et al. Diagnostic accuracy of the apparent diffusion coefficient in differentiating benign from malignant uterine endometrial cavity lesions: initial results. *Eur Radiol* 2008;18:384–9.
25. Namimoto T, Awai K, Nakaura T, Yanaga Y, Hirai T, Yamashita Y. Role of diffusion-weighted imaging in the diagnosis of gynecological diseases. *Eur Radiol* 2009; 19:745–60.
26. Tamai K, Koyama T, Saga T, Umeoka S, Mikami Y, Fujii S et al. Diffusion-weighted MR imaging of uterine endometrial cancer. *J Magn Reson Imaging* 2007;26:682–7.
27. Shen SH, Chiou YY, Wang JH, Yen MS, Lee RC, Lai CR et al. Diffusion-weighted single-shot echo-planar imaging with parallel technique in assessment of endometrial cancer. *AJR Am J Roentgenol* 2008;190:481–8.
28. Kilickesmez O, Bayramoglu S, Inci E, Cimilli T, Kayhan A. Quantitative diffusion-weighted magnetic resonance imaging of normal and diseased uterine zones. *Acta Radiol* 2009;50:340–7.
29. Inada Y, Matsuki M, Nakai G, Tatsugami F, Tanikake M, Narabayashi I et al. Body diffusion-weighted MR imaging of uterine endometrial cancer: is it helpful in the detection of cancer in nonenhanced MR imaging? *Eur J Radiol* 2009;70:122–7.
30. Takeuchi M, Matsuzaki K, Nishitani H. Diffusion-weighted magnetic resonance imaging of endometrial cancer: differentiation from benign endometrial lesions and preoperative assessment of myometrial invasion. *Acta Radiol* 2009;50: 947–53.
31. Anstee A, Scott F, Culver L, Rustin G, Padwick M, Padhani A. Diffusion-weighted MRI: Correlation with tumour grade in endometrial cancer and normal uterine tissues. *Eur Radiol* 2007.
32. Bokhman JV. Two pathogenetic types of endometrial carcinoma. *Gynecol Oncol* 1983;15:10–17.
33. Mendivil A, Schuler KM, Gehrig PA. Non-endometrioid adenocarcinoma of the uterine corpus: a review of selected histological subtypes. *Cancer Control* 2009;16:46–52.
34. Dunton CJ, Balsara G, McFarland M, Hernandez E. Uterine papillary serous carcinoma: a review. *Obstet Gynecol Surv* 1991;46:97–102.
35. Hricak H, Stern JL, Fisher MR, Shapeero LG, Winkler ML, Lacey CG. Endometrial carcinoma staging by MR imaging. *Radiology* 1987;162:297–305.
36. Barwick TD, Rockall AG, Barton DP, Sohaib SA. Imaging of endometrial adenocarcinoma. *Clin Radiol* 2006;61:545–5.
37. Nakamura K, Kodama J, Okumura Y, Hongo A, Kanazawa S, Hiramatsu Y. The SUVmax of ^{18}F -FDG PET correlates with histological grade in endometrial cancer. *Int J Gynecol Cancer* 2010;20:110–5.